Published in final edited form as:
Nat Chem. 2019 July ; 11(7): 669–675. doi:10.1038/s41557-019-0266-1.

A catalytically active [Mn]-hydrogenase incorporating a non-native metal cofactor

Hui-Jie Pan[1], **Gangfeng Huang**[2], **Matthew D. Wodrich**[1,3], **Farzaneh Fadaei Tirani**[1], **Kenichi Ataka**[4], **Seigo Shima**[2,*], and **Xile Hu**[1,*]

[1]Laboratory of Inorganic Synthesis and Catalysis, Institute of Chemical Sciences and Engineering, Ecole Polytechnique Fédérale de Lausanne (EPFL), ISIC-LSCI, BCH 3305, Lausanne 1015, Switzerland [2]Max Planck Institute for Terrestrial Microbiology, Karl-von-Frisch-Straße 10, 35043 Marburg, Germany [3]Laboratory for Computational Molecular Design, Institute of Chemical Science and Engineering, Ecole Polytechnique Fédérale de Lausanne (EPFL), Lausanne 1015, Switzerland [4]Department of Physics, Freie Universität Berlin, Arnimallee 14, Berlin 14195, Germany

Abstract

Nature carefully selects specific metal ions for incorporation into the enzymes that catalyze the chemical reactions necessary for life. Hydrogenases, enzymes that activate molecular H_2, exclusively utilize Ni and Fe in [NiFe]-, [FeFe]-, and [Fe]-hydrogeanses. However, other transition metals are known to activate or catalyze the production of hydrogen in synthetic systems. Here, we report the development of a biomimetic model complex of [Fe]-hydrogenase that incorporates a Mn, as opposed to a Fe, metal center. This Mn complex is able to heterolytically cleave H_2 as well as catalyze hydrogenation reactions. Incorporation of the model into an apoenzyme of [Fe]-hydrogenase results in a [Mn]-hydrogenase with enhanced occupancy-normalized activity over an analogous semi-synthetic [Fe]-hydrogenase. These findings represent the first instance of a non-native metal hydrogenase showing catalytic functionality and demonstrate that hydrogenases based on a manganese active site are viable.

*Correspondence to: shima@mpi-marburg.mpg.de; xile.hu@epfl.ch.

Data Availability. The authors declare that the data supporting the findings of this study are available from the corresponding authors upon reasonable request. CCDC-1856616 and CCDC-1856615 contain the supplementary crystallographic data for **3** and **4(18-crown-6)**, respectively. These data can be obtained free of charge from *The Cambridge Crystallographic Data Centre via* www.ccdc.cam.ac.uk/data_request/cif.

Author Contributions S.S. and X.L.H. directed the research. H-J.P. conducted the experiments of the Mn complexes; G.F.H conducted experiments of semisynthetic enzymes; M.D.W. did the computations; F.F.T. did the crystallographic study of Mn complexes; K.A. performed IR spectroscopy of enzymes; All authors discussed data. X.L.H. wrote the manuscript with contributions from H-J.P and S.S.

Competing interests The authors declare no competing interests.

Europe PMC Funders Author Manuscripts

Europe PMC Funders Author Manuscripts

Introduction

Nature judiciously chooses metal ions to catalyze biochemical reactions. Understanding these choices is not only important for fundamental knowledge of biocatalysis, but might also provide guidelines for designing synthetic catalysts. Structure-activity studies where native metal ions are replaced by non-native analogues represent a direct approach for unraveling the choices made by nature. However, abiological replacement of native metals that maintain the activity of the native enzyme activity have rarely been reported.1–3

When it comes to the activation of dihydrogen (H_2), nature chooses only Fe and Ni, as in [NiFe]-, [FeFe]-, and [Fe]-hydrogeanses.4 It is not yet clear whether this choice is due solely to the higher bioavailability of Fe and Ni relative to other metals, or due to their unique ability to activate H_2 in biological systems. Many other transition metals are known to activate or evolve hydrogen in synthetic systems. A [RuRu] analogue of [FeFe]-hydrogenase was the only semi-synthetic hydrogenase that contained a non-native metal, but it was inactive.5 [Fe]-hydrogenase is an attractive platform to address the questions concerning the choices of metals in biological H_2 activation.6 This enzyme catalyzes the hydrogenation of methenyl-tetrahydromethanopterin (methenyl-H_4MPT$^+$) to form methylene-H_4MPT, a reaction involved in microbial methanogenesis.7 Unlike [NiFe]- and [FeFe]-hydrogenases, [Fe]-hydrogenase has only one Fe center per active site. In its resting state, the low-spin Fe^{II} center is coordinated by one H_2O and two cis-CO molecules, a cysteine-thiolate, as well as an acyl carbon and a pyridinyl nitrogen from a guanylylpyridinol moiety (Fig. 1a).8,9 During catalysis, water likely dissociates, thereby opening a binding site for H_2. Considering that Mn(I) and Fe(II) are isoelectronic, and further inspired by the recent development of Mn-catalyzed hydrogenation,10 we decided to prepare a Mn(I) model of the active site of [Fe]-hydrogenase. Through reconstitution of the apoenzyme of [Fe]-hydrogenase with this Mn(I) model, we have obtained the first [Mn]-hydrogenase. This artificial hydrogenase is active for the native [Fe]-hydrogenase reactions, indicating Mn as a viable metal for biological H_2 activation in the enzyme.

Results

Synthesis, characterization, and catalytic activity of Mn models

The reaction of *2*-hydroxy-*6*-methylpyridine (**1**) with two equivalents of *n*-BuLi gave a dilithiated intermediate (**2**), which was not isolated but treated directly with $Mn(CO)_5Br$ followed by acidic workup to give the targeted Mn(I) model **3** (Fig. 1b). The infrared (IR) spectrum of **3** in tetrahydrofuran (THF) exhibits four CO peaks at 1948, 1967, 1983 and 2068 cm^{-1} (Supplementary Fig. 13), indicative of a Mn tetra(carbonyl) species. The peak at 1651 cm^{-1} was attributed to the acyl group. The NMR spectra of **3** (in deuterated THF) is characteristic of a diamagnetic species (Supplementary Fig. 8), indicating a low-spin configuration of Mn(I). The *2*-OH proton gave a broad ^1H peak at 11.26 ppm. In the ^{13}C NMR spectrum [in deuterated acetonitrile (CD_3CN)] (Supplementary Fig. 9), three types of CO carbon were observed at 213.6, 215.9, and 220.3 ppm, respectively. The acyl carbon gave a peak at 280.8 ppm. CO/^{13}CO exchange was observed by ^{13}C NMR when **3** was treated with an excess of ^{13}CO in deuterated THF or CD_3CN, suggesting that one or more CO ligands readily dissociate from the Mn center (Supplementary Fig. 1-2). The solid-state

molecular structure of **3** was determined by X-ray crystallography (Fig. 1c). The Mn ion possesses an octahedral coordination geometry. Three CO ligands are co-planar, while the fourth CO ligand occupies a position orthogonal to the other three. The acylmethylpyridinol ligand coordinates in a bidentate fashion via the acyl C and pyridonal N.

A H_2/D_2 exchange assay was employed to test the activity of **3** towards H_2 activation.11 The reaction was conducted in a high-pressure NMR tube, where D_2 (8 bar) and H_2 (12 bar, total pressure of mixed gas 20 bar) were added to a solution of **3** in THF-*d*8. The reaction was monitored by NMR spectroscopy. Complex **3** alone did not mediate H/D exchange after two days at 25 °C. However, in the presence of a base (e.g., *1*-methylpyrrolidine (MP) or triethylamine (Et_3N)), the formation of HD was observed within 3 h at 25 °C (Supplementary Fig. 3), indicating H_2 activation. A D_2/H^+ exchange experiment was then conducted, in which 20 bar of D_2 was introduced to a CD_3CN-*d3* solution of **3** containing 3.0 equivalent of MP at 25 °C. H_2 and HD were detected after 1 h (Supplementary Fig. 5). This result indicates that H_2 splitting is a heterolytic process, which is the same as in the enzymatic reaction.

We previously reported that deprotonation of the *2*-OH group was a key step in enabling H_2 activation by a semi-synthetic [Fe]-hydrogenase.12 After deprotonation, the anionic *2*-O^- group served as an internal base to assist in the heterolytic splitting of H_2 at the Fe center. 12,13 The need for a base for H_2 splitting by **3** suggested that a similar mechanism was operating in the activation of H_2 by **3**. To verify this hypothesis, we sought to intentionally deprotonate the *2*-OH group in **3**. A clean reaction was observed upon treatment of **3** with potassium hydride (KH) in THF at room temperature (Fig. 1d). In the ^1H NMR spectrum of the *in-situ* formed complex **4**, all the peaks of **3** except the *2*-OH peak were still observed, with a significant upfield shift (Supplementary Fig. 10). ^1H NMR spectra similar to that of **4** were obtained when **3** was treated with an excess of MP or Et_3N, suggesting the formation of a similar deprotonated species. To facilitate isolation and crystallization, **4** was treated with a K^+-selective crown ether, 18-crown-6 to give complex **4**(18-crown-6) (Fig.1d). **4** and **4**(18-crown-6) exhibit similar NMR spectra (Supplementary Fig. 10-11). The IR spectrum of **4**(18-crown-6) in THF exhibits four ν(CO) peaks at 1901, 1944, 1972, 2052 cm^{-1}, and a ν(acyl C=O) peak at 1616 cm^{-1} (Supplementary Fig. 14). These peaks are shifted to lower values compared to the corresponding peaks in **3**, indicating a more electron-rich Mn center upon deprotonation of the *2*-OH group. The X-ray structure of **4**(18-crown-6) confirmed the deprotonation of the *2*-OH group (Fig. 1e). The *2*-O^- group has a strong interaction (2.6097(14) Å) with the K cation, which is further coordinated by the 6 O atoms of 18-crown-6. Both **4** and **4**(18-crown-6) were able to activate H_2 without an external base, as observed in the H_2/D_2 exchange assay (Supplementary Fig. 4). This result supports that deprotonation of *2*-OH group is a key step in H_2 activation by **3** in the presence of a base.

Complexes **3** and **4** are hydrogenation catalysts. To optimize the reaction conditions, hydrogenation of benzaldehyde (**5a**) was employed as a test reaction with complex **3** as the catalyst. After screening various reaction parameters, the best conditions were: 1 mol% complex **3** with 20 mol% MP as base under 50 bar H_2 at 80 °C in THF (Fig. 1f). Under these conditions, the yield of hydrogenation was quantitative. Although H_2 activation was

observed at 25 °C, a higher temperature (*e.g.*, 80 °C) was necessary for catalytic hydrogenation, suggesting that hydride transfer was more difficult than H_2 activation. Under similar conditions using **4** (5 mol%) rather than **3** as the catalyst and without the base, hydrogenation was also achieved in a 96% yield. Similar reaction conditions could be applied for the hydrogenation of other substrates including: ketone (**5b**), primary imine (**5c**), and secondary imine (**5d**; Fig. 1g), moderate yields were obtained (Supplementary Fig. 6). The hydrogenation of an olefin substrate was less efficient (**5e**; Fig. 1g). The reaction profiles of hydrogenation reactions were monitored by ^{19}F NMR spectroscopy using *4*-CF_3 benzaldehyde (**5f**) as the substrate (Supplementary Fig. 7). No induction period was observed, suggesting that **3** and **4** were the true pre-catalysts or catalysts. The initial rates of reactions catalyzed by **3** and **4** were similar, but the reaction catalyzed by **4** was slower, probably due to some decomposition of **4**. The catalytic activity of **3** for hydrogenation is modest compared to some state-of-the-art Mn and Fe catalysts (Supplementary Table 2). The ligand environment of **3** is less electron donating than those of highly active Mn complexes, leading to a less hydridic Mn-H intermediate, which might be the origin of the subdued activity.

Density functional theory (DFT) computations (PBE0-dDsC/TZ2P//M06/def2-SVP theoretical level, see Computational Methods in Supplementary Information) suggest the following catalytic cycle for the hydrogenation of **5a** catalyzed by **3** (Fig. 2a and Supplementary Fig. 21). Deprotonation of the *2*-OH group in **3** by the base MP followed by substitution of one CO ligand (trans to the acyl ligand) by H_2 gives intermediate **7b**. Heterolytic cleavage of the coordinated H_2 in **7b** leads to a hydride complex **7c**, which hydrogenates **5a** to give the alcohol-bound complex **7e**. Replacing the alcohol product in **7e** by H_2 yields the product and regenerates **7b**. The substitution of CO in **7a** by H_2 as well as the transition state associated with hydride transfer represent the highest points on the potential energy surface (Fig. 2b), with similar values of about 26 kcal/mol. Deprotonation and H_2 splitting are facile processes. Given the accuracy of the DFT method, the computed reaction energy profile qualitatively agrees with the experimental results.

Reconstitution and activity of [Mn]-hydrogenase

The activity of **3** in H_2 splitting and hydrogenation catalysis contrasts the inactivity of its Fe(II) analogue in H_2 activation.12 This reactivity difference is consistent with recent observations that Mn(I) complexes are often more active or stable than Fe(II) complexes in hydrogenation reactions.10 However, it was unclear whether Mn would be competent for biological H_2 activation. The study of semi-synthetic [RuRu]-hydrogenase showed that even though H_2 activation on synthetic Ru complexes was facile, in a hydrogenase environment this metal was inactive.5 To test possible Mn-catalyzed hydrogenase activity, complex **3** was employed to reconstitute a [Mn]-hydrogenase. The protocol previously used for the reconstitution of semi-synthetic [Fe]-hydrogenases was also applicable here.12 **3** was first dissolved in a solution containing 99% methanol and 1% of acetic acid. The solution containing two equivalents of **3** was mixed with a solution of [Fe]-hydrogenase apoenzyme from *Methanocaldococcus jannaschii* heterologously produced in *Escherichia coli* in the presence of 2-mM GMP (GMP = guanosine monophosphate). While **3** is soluble in pure methanol, active enzyme was not reconstituted using a methanol solution of **3** in the absence

of acetic acid. The role of acetic acid is unclear as the IR spectra of complex **3** in pure methanol and in mixtures of methanol and acetic acid are essentially the same (Supplementary Fig. 15-16), suggesting that an acetate-bound form of **3** was not the major species in the reconstitution medium as was the case for the reconstitution of semisynthetic [Fe]-hydrogenase.12

The activity of this [Mn]-hydrogenase was measured photometrically for both the forward (reduction of methenyl-H_4MPT^+ with H_2) and the reverse (H_2 production from methylene-H_4MPT) reactions. The absorbance of methenyl- H_4MPT^+ at 336 nm was used as a spectroscopic probe of the reaction rate. To our delight, the [Mn]-hydrogenase was active for the native reactions of [Fe]-hydrogenase (Fig. 3a-d). The activity largely remained identical for multiple samples; the averaged apparent specific activity was 1.5 ± 0.1 U/mg and 0.09 ± 0.01 U/mg for the forward and reverse reaction, respectively. As observed in the reconstitution of semisynthetic [Fe]-hydrogenase,12 the absence of GMP in the reconstitution solution resulted in a 2-fold decrease of the activity of the reconstituted enzyme (Table 1) although the IR spectrum was not changed (Supplementary Fig. 17). Interestingly, the [Mn]-hydrogenase is biased towards the forward reaction, which is around 20 times faster than the reverse reaction. The native [Fe]-hydrogenase and semi-synthetic [Fe]-hydrogenase have only slightly higher rates for the forward reaction (Table 1).12,14 The forward reaction was conducted at pH 7.5 while the reverse reaction was conducted at pH 6.0. The bias of the [Mn]-hydrogenase toward the forward reaction might be due to the higher pKa of the 2-OH group compared to [Fe]-hydrogenase and semi-synthetic[Fe]-hydrogenase,12 which hinders its deprotonation at pH 6.0, thereby decreasing the base function and the rate of the reverse reaction. Control experiments showed that complex **3** or the apoenzyme of [Fe]-hydrogenase alone did not afford the activity.

In [Fe]-hydrogenase, the Fe center is bound to Cys176 thiolate. The reconstituted Cys176Ala variant of [Mn]-hydrogenase has a specific activity of 0.12±0.19 U/mg for the forward reaction, which is 8% of the native variant of the reconstituted [Mn]-hydrogenase. This result contrasts the findings on semi-synthetic [Fe]-hydrogenase, where reconstituted Cys176Ala variants were inactive (Table 2).12 This suggests that binding of the Mn complex to Cys176-S is not absolutely needed for [Mn]-hydrogenase to be active. In the native [Fe]-hydrogenase, the iron complex component of the FeGP cofactor is connected to the protein via hydrogen bonds involving the backbone NH of Cys176, the hydroxyl group of Thr13, the carboxy group of Asp251, and water molecules (Supplementary Fig. 18). These interactions might lead to specific binding of the Mn complex even in the absence of Cys176-Fe bonding, albeit with an unoptimized orientation.

Different batches of samples of [Mn]-hydrogenase have nearly identical activity, however, they exhibit different IR spectra in the region of ν(CO) vibrational bands. For example, the spectral shape and positions of two samples are similar and resemble those of complex **3** (Supplementary Fig. 19a-b) but their intensities are different. A third sample has a spectrum similar to that of native [Fe]-hydrogenase (Supplementary Fig. 19). This result suggests that various amount of Mn complexes are unspecifically bound to the protein in different samples in addition to a similar amount of specifically bound complex, which gives rises to the hydrogenase activity. Assuming that the IR spectrum of Figure S19c originates from

specifically bound Mn mimic because only two CO bands at 1985 and 1965 cm^{-1} were detected, we estimated the occupancy of the active site of [Mn]-hydrogenase as 20%, by comparing its CO peak area with that of the reconstituted native [Fe]-hydrogenase (Supplementary Fig. 19). Considering this occupancy, the actual specific activity is about 7.5 U/mg (forward reaction) and 0.45 U/mg (reverse reaction). The corresponding turnover frequencies (TOFs) are 5 s^{-1} and 0.3 s^{-1} for the forward and reverse reactions, respectively. These TOFs are 3 orders of magnitude higher than those of complex **3** alone in hydrogenation reactions (Supplementary Table 3), underscoring the important role of the protein environment for catalysis. They are also significantly higher than those of state-of-the-art synthetic Mn and Fe catalysts (Supplementary Table 3).

To probe whether the unspecifically bound Mn complex contributed to the activity of [Mn]-hydrogenase, reconstitution was conducted using a mutated apoenzyme of [Fe]-hydrogenase, in which the binding residues for the FeGP cofactor were triply mutated (T13V, C176A and D251A). Although unspecific binding of complex **3** to the triple mutant apoenzyme was confirmed by IR spectroscopy (Supplementary Fig. 20), this variant of [Mn]-hydrogenase had no enzymatic activity (Table 2). Moreover, F_{420}-dependent methylene-H_4MPT dehydrogenase (Mtd), which does not bind the FeGP cofactor but binds the H_4MPT substrates, was also used for reconstitution. Unspecific binding of complex **3** by Mtd was again observed (Supplementary Fig. 20), but this sample also showed no enzymatic activity (Table 2). Taken together, these data indicate that the unspecific bound Mn complex is catalytically inactive.

Discussion

The active sites of both the semi-synthetic [Mn]- and [Fe]-hydrogenase lack the guanosine monophosphate (GMP) moiety and two methyl groups in the pyridinol group of the native cofactor (Fig. 1a), which should be the principle reason for their specific activity being only a few percent of native [Fe]-hydrogenase.12 Direct comparison of the semi-synthetic [Mn]- and [Fe]-hydrogenases, however, reveals the relative catalytic competency of the two different metals. The occupancy-normalized specific activity of [Mn]-hydrogenase is 25% higher than in the analogous [Fe]-hydrogenase for the forward reaction (3 U/mg at 50% active site occupancy),12 which is the physiological reaction during methanogenesis. Thus, Mn appears to be more active than Fe for enzymatic H_2 activation.

In summary, a Mn(I) model of the active site of [Fe]-hydrogenase that is capable of splitting H_2 and catalyzing hydrogenation reactions has been prepared. Reconstitution of the apoenzyme of [Fe]-hydrogenase with this Mn(I) model leads to a [Mn]-hydrogenase, which is active for the [Fe]-hydrogenase reactions. These findings represent the first demonstration of catalytic functionality of a non-native metal in a hydrogenase enzyme. The molar activity of this semi-synthetic [Mn]-hydrogenase is higher than its Fe analogue, raising an intriguing question – why does nature choose Fe over Mn?

Methods

Synthesis of complex 3

2-Hydroxy-*6*-Methylpyridine **1** (1.3 g, 12 mmol) was dissolved in 60 mL of dry THF in a Schlenk flask. To this solution, *n*-BuLi (2.5 M in hexane, 9.6 mL, 24 mmol) was added dropwise at 0 °C and the solution was further stirred for 30 min at 0 °C. In another schlenk flask a THF (80 mL) solution of $Mn(CO)_5Br$ (3.3 g, 12 mmol) was cooled to -78 °C. The solution of deprotonated **1** was then added dropwise to the $Mn(CO)_5Br$ solution at -78 °C. The resulting mixture was allowed to slowly warm to room temperature and further heated to 50 °C. After stirring at 50 °C overnight, the mixture was cooled to room temperature and 1.5 mL of 37% HCl aqueous solution was then slowly added. THF solvent was removed 30 min later. The residue was further purified by silica gel chromatography in glovebox (1.3 g, 36%) using ethyl acetate/hexane as eluent. Single crystal suitable for X-ray test was obtained via layer diffusion of pentane to a THF solution of complex **3** at -22 °C.

Synthesis of complex 4 and 4(18-crown-6)

To a solution of complex **3** (1.0 g, 3.3 mmol) in THF (5 mL) was added KH (132 mg, 3.3 mmol) slowly under stirring at room temperature. When there was no more H_2 gas formed, a THF solution of 18-crown-6 (958 mg, 3.6 mmol) was added at once to the mixture. The resulting mixture was further stirred at room temperature for 2 h before it was filtered through a Teflon membrane to remove all the solid impurity. A layer of Et_2O was then added on top of the THF solution and the mixture was stored at -22 °C. Crystal of **4(18-crown-6)** was obtained in 75% yield (1.5 g).

Computational methods

The geometries of all species were optimized at the M06/def2-SVP theoretical level using the “ultrafine” integration grid and the SMD implicit solvent model for tetrahydrofuran as implemented in Gaussian09. Refined energy estimates were obtained using single point computations on the optimized M06 geometries at the PBE0-dDsC/TZ2P level as implemented in ADF. Reported free energies are derived from the PBE0-dDsC electronic energies, M06 enthalpy and vibrational only entropy contributions, and solvation corrections using the COSMO-RS model.

Preparation of apoenzymes

The [Fe]-hydrogenase-encoding gene (*hmd*) from *M. jannaschii*8 and the gene encoding F_{420}-dependent methylene-H_4MPT dehydrogenase (*mtd*) gene from *Archaeoglobus fulgidus*15. The complete genome sequence of the hyperthermophilic, sulphate-reducing archaeon *Archaeoglobus* fulgidus were cloned into the expression vector pET24b. Genes of the *hmd* mutants (C176A and T13V-C176A-D251A) were synthesized using the template of the wild type *hmd* gene by GenScript. The *E. coli* strain BL21(DE3) containing the expression vector for *hmd* or *mtd* was cultivated and the gene expression was induced. The over-produced protein was purified as described previously8.

Reconstitution of [Mn]-hydrogenase

Complex **3** was dissolved in solution containing 99% methanol and 1% acetic acid. The reconstitution of [Mn]-hydrogenase was performed in the anaerobic tent (95% N_2/5% H_2) at 8 °C. The 2 ml reconstituted system contains 0.5 mM complex **3**, 0.25 mM apoenzyme, 2 mM guanosine monophosphate (GMP) and 100 mM sodium acetate buffer pH 5.6. The mixture was incubated on ice for 1 h. Then the mixture was washed by 10 mM MOPS/KOH pH 7.0 containing 2 mM DTT through a 30 kDa cut-off ultrafilter with at least totally1000 folds dilution to remove the unbound complex **3**. Finally, the reconstituted [Mn]-hydrogenase holoenzyme was concentrated to ~50 mg/ml for enzyme activity assay. The reconstituted enzyme was quickly frozen in liquid nitrogen and store at –75 °C. The reconstitution of semisynthetic [Mn]-hydrogenase using the mutated apoenzyme and Mtd, and semisynthetic [Fe]-hydrogenases were performed using the same method in the presence of 2 mM GMP as described above. The native [Fe]-hydrogenase with the FeGP cofactor was prepared as described previously.8

Enzyme activity assay of the [Mn]-hydrogenase holoenzyme

The reduction of methenyl-tetrahydromethanopterin (methenyl-H_4MPT^+) to methylene-H_4MPT (the forward reaction) and the dehydrogenation of methylene-H_4MPT to methenyl-H_4MPT^+ (the reverse reaction) was measured. For the forward reaction, 20 μM (final concentration) methenyl-H_4MPT^+ was added to a 0.7 ml solution containing 120 mM potassium phosphate buffer pH 7.5 containing 1 mM EDTA under 100% H_2 gas phase at 40 °C. The reaction was started by injecting 10 μl reconstituted [Fe]-hydrogenase sample. Reduction of methenyl-H_4MPT^+ was detected by measuring the decrease of the absorbance at 336 nm. For the reverse reaction, 20 μM (final concentration) methylene-H_4MPT was added to a 0.7 ml solution containing 120 mM potassium phosphate buffer pH 6.0 containing 1 mM EDTA under a 100% N_2 gas phase at 40 °C. The reaction was started by injecting 10 μl reconstituted [Mn]-hydrogenase sample. Dehydrogenation of methylene-H_4MPT was detected by measuring the increase in the absorbance at 336 nm. The activities were calculated using the extinction coefficient of methenyl-H_4MPT^+ ($\varepsilon_{336\ nm}$ = 21.6 $mM^{-1}cm^{-1}$).14 One unit (U) activity is the amount of enzyme catalyzing the decrease of 1 μmol/min methenyl-H_4MPT^+ (the forward reaction) or increase of methenyl-H_4MPT^+ (the reverse reaction). For the kinetic measurements shown in Fig.3, the absorbance was measured with an Ultrospec 1100pro spectrophotometer (GE Healthcare); the spectra were recorded on a Specode S600 diode-array spectrophotometer (Jena Analytik). The 20 μM methenyl-H_4MPT^+ and 20 μM methylene-H_4MPT (final concentration) was used as the substrate for the forward and reverse reaction, respectively, 0.007 mg/ml reconstituted enzyme (final concentrations) was added to the 0.7 ml reaction mixture; the light path of the cuvette was 1 cm. The spectra were recorded every 10 s. As a control, complex **3** (14 uM, final concentration) or the apoenzyme (0.014 mg/ml) was added to the assay instead of the reconstituted enzyme.

Infrared spectroscopy of enzyme

The samples for IR spectroscopy were prepared in amber-colored 1.5-ml Eppendorf tubes. The sample solutions contained 150 mg/ml (4-mM) semisynthetic [Mn]-hydrogenase in 10-

mM MOPS/NaOH pH 7.0. The sample solutions were prepared in the anaerobic tent with the gas phase 95%N_2/5%H_2 and then frozen in liquid nitrogen. The frozen samples in tubes were stored in a Dewar filled with liquid nitrogen until the measurements were taken.

All IR spectra were obtained with an FTIR spectrometer (Bruker, Vertex 70V) in an attenuated total reflection (ATR) optical configuration with a Si prism of 45° incident angle and 2 active reflections (Smith Detection, DuraSamplIR IITM). Spectra were obtained with a resolution of 4 cm^{-1}. Five micro-litres of the sample solutions were dropped onto the effective area of a Si prism (3 mm diameter) and concentrated by slowly evaporating the solvent under mild flow of argon gas. The hydration of the sample was estimated by the relative intensities of the water band (OH stretching mode) at approximately 3500 cm^{-1} against the amide II band of the protein at approximately 1550 cm^{-1}. Spectra were measured successively during the concentration process. We selected a spectrum of a mildly hydrated sample that provided enough intensity to analyze the cofactor bands. A baseline correction was made on the selected spectrum to eliminate contributions of the broad background from the water overtone band at approximately 2000 cm^{-1}. Typically, 512 spectra were averaged to obtain a sufficient signal-to-noise ratio. Measurements were performed in the dark by covering the spectrometer with blackout fabric to avoid light-induced decomposition of the sample. Intensities of the observed bands from various samples were at arbitrary concentrations. For quantitative comparison of the obtained spectra, intensities of the CO bands were normalized by the peak intensities of the amide II band of each spectrum.

Supplementary Material

Refer to Web version on PubMed Central for supplementary material.

Acknowledgements

This work was supported by the Swiss National Science Foundation (to X.L.H), European Union Marie Sklodowska-Curie Individual Fellowships (794000 to H-J.P), Max Planck Society (to S.S.) and Deutsche Forschungsgemeinschaft (SH 87/1-1, to S.S.). M.D.W. acknowledges C. Corminboeuf (EPFL)for financial support and the Laboratory for Computational Molecular Design (EPFL) for providing computing resources. G.H. was supported by a fellowship from the China Scholarship Council (CSC). Correspondence and requests for materials should be addressed to S.S or X.L. H

References

1. Coleman JE. Metal ion dependent binding of sulphonamide to carbonic anhydrase. Nature. 1967; 214:193–194. [PubMed: 4962206]
2. Cuatrecasas P, Fuchs S, Anfinsen CB. Catalytic properties and specificity of the extracellular nuclease of Staphylococcus aureus. Journal of Biological Chemistry. 1967; 242:1541–1547. [PubMed: 4290246]
3. Schwizer F, et al. Artificial Metalloenzymes: Reaction Scope and Optimization Strategies. Chemical Reviews. 2018; 118:142–231. [PubMed: 28714313]
4. Lubitz W, Ogata H, Rudiger O, Reijerse E. Hydrogenases. Chem Rev. 2014; 114:4081–4148. [PubMed: 24655035]
5. Sommer C, Richers CP, Lubitz W, Rauchfuss TB, Reijerse EJ. A [RuRu] Analogue of an [FeFe]-Hydrogenase Traps the Key Hydride Intermediate of the Catalytic Cycle. Angewandte Chemie International Edition. 2018; 57:5429–5432. [PubMed: 29577535]
6. Shima S, Ermler U. Structure and Function of [Fe]-Hydrogenase and its Iron-Guanylylpyridinol (FeGP) Cofactor. European Journal of Inorganic Chemistry. 2011:963–972.

7. Thauer RK, Kaster AK, Seedorf H, Buckel W, Hedderich R. Methanogenic archaea: ecologically relevant differences in energy conservation. Nat Rev Microbiol. 2008; 6:579–591. [PubMed: 18587410]

8. Shima S, et al. The crystal structure of [Fe]-hydrogenase reveals the geometry of the active site. Science. 2008; 321:572–575. [PubMed: 18653896]

9. Hiromoto T, et al. The crystal structure of C176A mutated [Fe]-hydrogenase suggests an acyl-iron ligation in the active site iron complex. FEBS Letters. 2009; 583:585–590. [PubMed: 19162018]

10. Kallmeier F, Kempe R. Manganese Complexes for (De)Hydrogenation Catalysis: A Comparison to Cobalt and Iron Catalysts. Angewandte Chemie - International Edition. 2018; 57:46–60. [PubMed: 29065245]

11. Xu T, et al. A Functional Model of Fe -Hydrogenase. Journal of the American Chemical Society. 2016; 138:3270–3273. [PubMed: 26926708]

12. Shima S, et al. Reconstitution of [Fe]-hydrogenase using model complexes. Nature Chemistry. 2015; 7:995–1002.

13. Wodrich MD, Hu X. Natural inspirations for metal–ligand cooperative catalysis. Nature Reviews Chemistry. 2017; 2

14. Zirngibl C, et al. H-2-Forming Methylenetetrahydromethanopterin Dehydrogenase, a Novel Type of Hydrogenase without Iron-Sulfur Clusters in Methanogenic Archaea. European Journal of Biochemistry. 1992; 208:511–520. [PubMed: 1521540]

15. Klenk H-P, et al. The complete genome sequence of the hyperthermophilic, sulphate-reducing archaeon Archaeoglobus fulgidus. Nature. 1997; 390:364. [PubMed: 9389475]

Europe PMC Funders Author Manuscripts

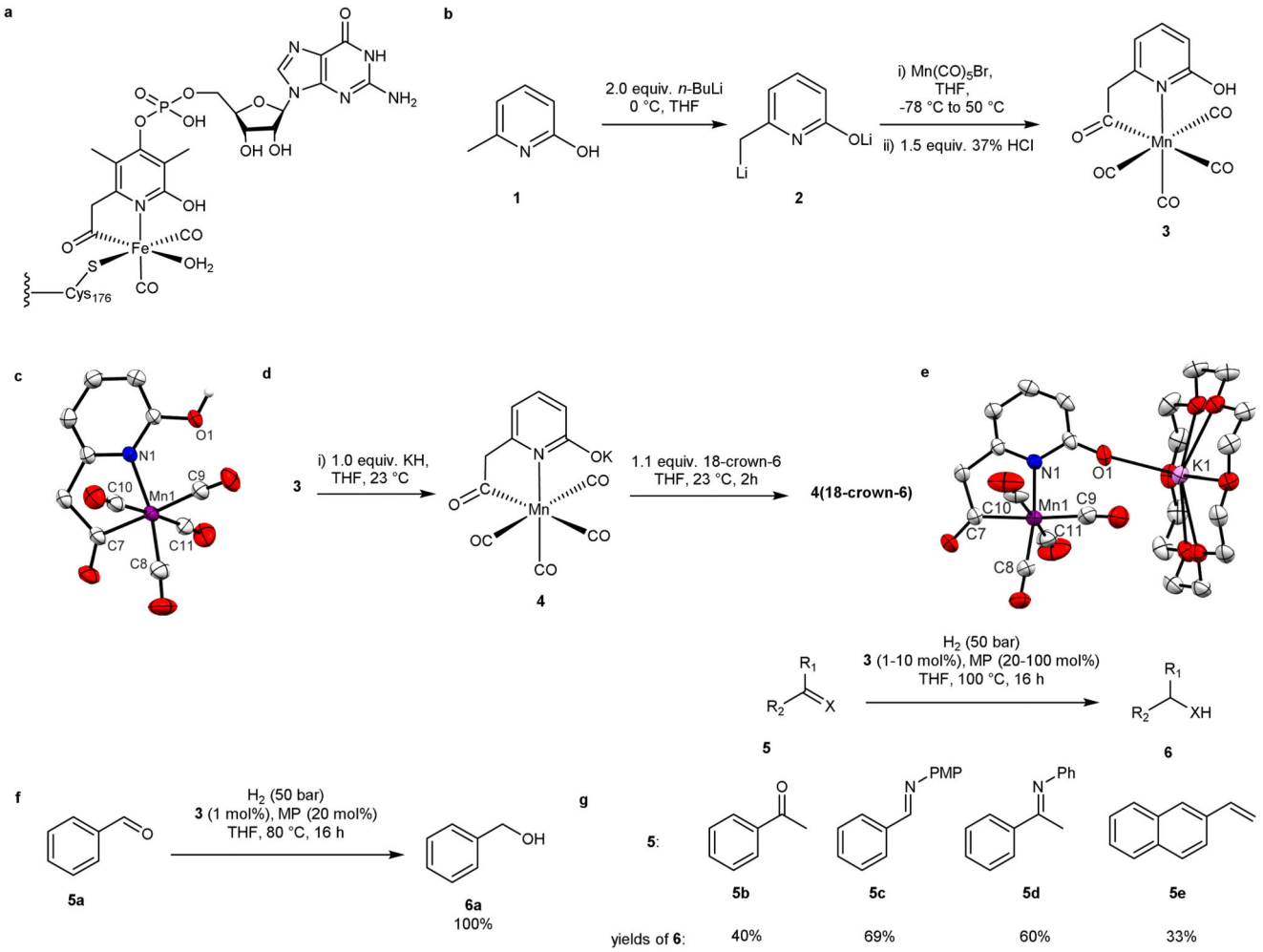

Figure 1. Active site of [Fe]-hydrogenase and synthesis, structure, and catalytic activity of its Mn models.

(a) The active site in [Fe]-hydrogenase. (b) Synthesis of complex **3** which is a non-native metal mimic of the active site of [Fe]-hydrogenase. (c) X-ray structure of complex **3**; thermal eliposoids are displayed at a 50% probability; (d) Synthesis of complexes **4** and **4(18-crown-6)** which are deprotonated forms of **3**; the reactions prove that the 2-OH group in **3** is prone to deprotonation. (e) X-ray structure of complex **4(18-crown-6)** confirming the deprotonation of the 2-OH group. Thermal eliposoids are displayed at a 50% probability. (f) Optimized conditions for the hydrogenation of benzaldehyde. (g) Other suitable substrates for catalytic hydrogenation. See Supplementary Fig. 6 for experimental details. PMP = *para*-methoxylphenyl; Ph = phenyl. Complex **3** is a catalyst for hydrogenation of various unsaturated organic compounds.

Europe PMC Funders Author Manuscripts

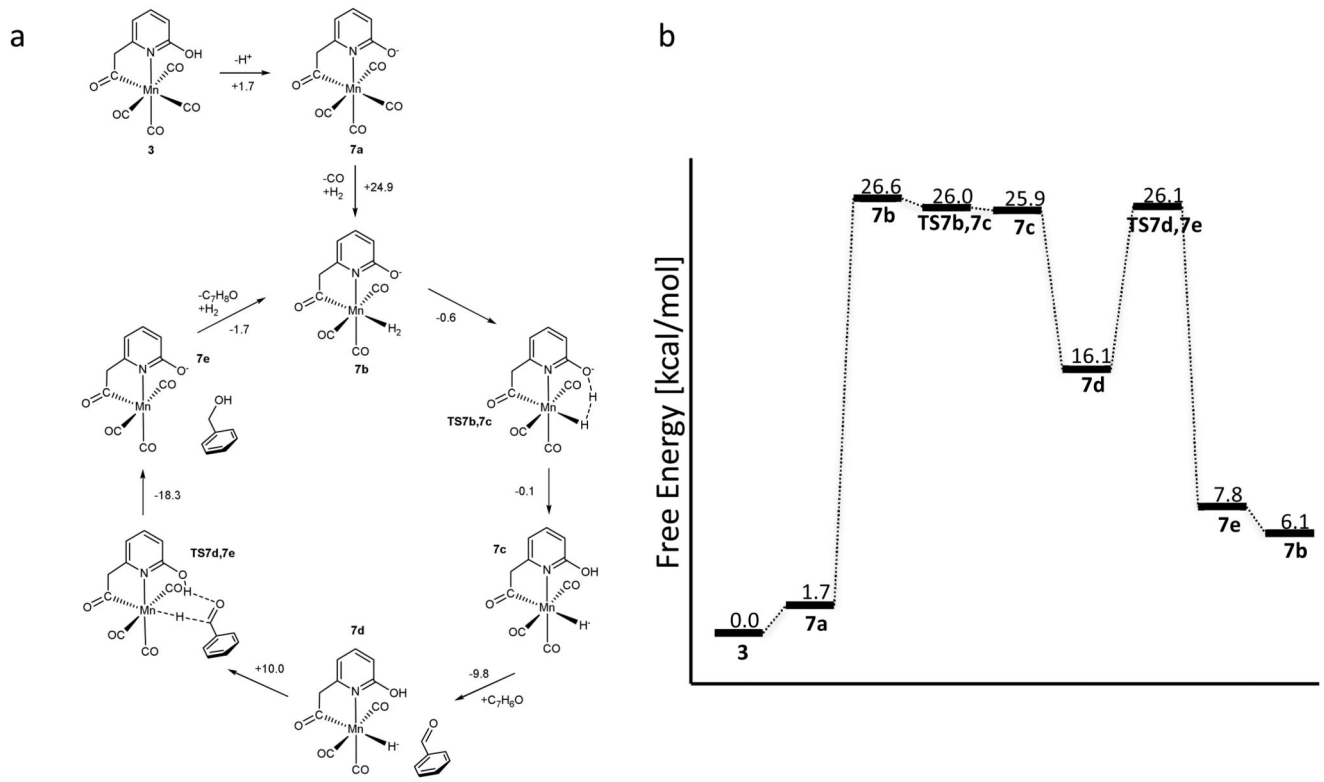

Figure 2. Computational study of the mechanism of hydrogenation.

(a) A DFT-computed (PBE0-dDsC/TZ2P//M06/def2-SVP level, see Computational Methods in the SI) catalytic cycle for the hydrogenation of **5a** catalyzed by **3**. The change of free energies is marked for each step. The catalysis follows the following sequence: deprotonation of the *2*-OH group of **3**, substitution of a CO ligand by H_2, heterolytic H_2 cleavage, binding of aldehyde, hydride and proton transfer to aldehyde, and finally substitution of bound alcohol by H_2. The Deprotonation of the *2*-OH group enables heterolytic H_2 splitting. (b) The reaction pathway and its associated free energy profile. The turnover limiting step is either the CO dissociation or the hydride transfer.

Europe PMC Funders Author Manuscripts

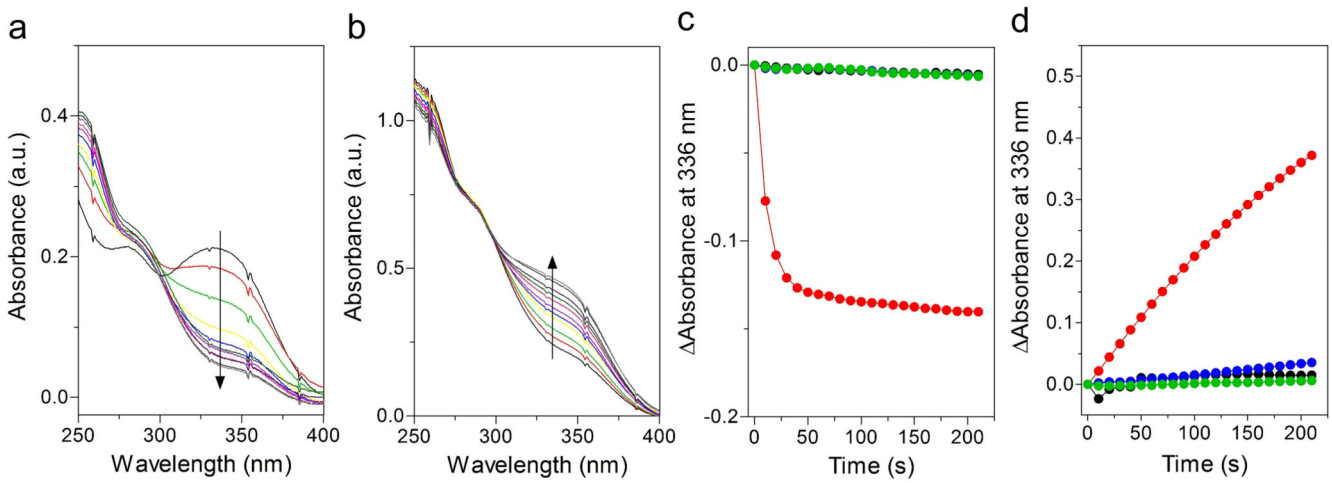

Figure 3. Activity of the semi-synthetic [Mn]-hydrogenase.

The consumption (a) and formation (b) of methenyl-H_4MPT^+ were detected (direction of the reactions is indicated by arrows); the changes of absorbance at 336 nm of the consumption (c) and formation (d) reactions are plotted. The red line shows activity with the reconstituted enzyme with complex **3**. As negative controls, the apoenzyme alone (black), complex **3** alone (blue) and only the buffer solution (green) were also tested. The black and blue traces in (c) are covered by the green trace. The increase of the absorbance of the sample with only **3** in (d) was due to an increase of turbidity caused by aggregation of the Mn complex in the assay, which was confirmed by the change of the overall UV-Vis spectrum. The data show that only [Mn]-hydrogenase, but not control samples, has substantial catalytic activity.

Europe PMC Funders Author Manuscripts

Table 1

Comparison of enzyme activity of native [Fe]-hydrogenase, reconstituted [Fe]-hydrogenase, semisynthetic [Fe]-hydrogenase and semisynthetic [Mn]-hydrogenase.

Samples	Specific activity (U/mg) (Forward reaction: reduction of methenyl-H_4MPT with H_2)		Specific activity (U/mg) (Reverse reaction: dehydrogenation of methylene-H_4MPT)	
	+ GMP[5]	− GMP[6]	+ GMP	− GMP
Native [Fe]-hydrogenase[1]	NA[7]	520 ± 30	NA	470 ± 10
Reconstituted [Fe]-hydrogenase[2]	NA	370 ± 20	NA	340 ± 40
Semisynthetic [Fe]-hydrogenase[3]	2.5 ± 0.4	1.2 ± 0.3	1.9 ± 0.2	1.0 ± 0.1
Semisynthetic [Mn]-hydrogenase[4]	1.5 ± 0.1	0.67 ± 0.10	0.09 ± 0.01	0.08 ± 0.02

The error bars represent standard deviation.

[1]Native [Fe]-hydrogenase: The purified [Fe]-hydrogenase from *Methanothermobacter marburgensis*.

[2]Reconstituted [Fe]-hydrogenase: [Fe]-hydrogenase was reconstituted using the Hmd apoenzyme from *Methanocaldococcus jannaschii* heterologous expressed in *E. coil* and the FeGP cofactor extracted from native [Fe]-hydrogenase from *M. marburgensis*.

[3]Semisynthetic [Fe]-hydrogenase: [Fe]-hydrogenase was reconstituted using from *Methanocaldococcus jannaschii* heterologous expressed in *E. coil* with an Fe-model complex.12

[4]Semisynthetic [Mn]-hydrogenase: Reconstituted apoenzyme of [Fe]-hydrogenase from *Methanocaldococcus jannaschii* heterologous expressed in *E. coil* with Mn-model complex **3**.

[5]+GMP: reconstitution solution contains 2 mM GMP.

[6]–GMP: reconstitution solution does not contain GMP.

[7]NA: not applicable.

Table 2

Comparison of enzyme activity of wild-type enzyme reconstituted with the FeGP cofactor (FeGP), semisynthetic [Fe]-hydrogenases, and semisynthetic [Mn]-hydrogenases reconstituted using wild-type and mutated Hmd apoenzymes from *Methanocaldococcus jannaschii* as well as F_{420}-dependent methylene-tetrahydromethanopterin dehydrogenase (Mtd) from *Archaeoglobus fulgidus*. Mtd binds methenyl- and methylene-tetrahydromethanopterin as substrates but does not use the FeGP cofactor.

Samples	**Specific activity (U/mg) (Forward reaction: reduction of methenyl-H_4MPT+ with H_2)**	**Specific activity (U/mg) (Reverse reaction: dehydrogenation of methylene-H_4MPT)**
Wild type enzymes reconstituted with		
FeGP	370 ± 20	340 ± 40
[Fe]	2.5 ± 0.4	1.9 ± 0.2
[Mn]	1.5 ± 0.1	0.09 ± 0.01
Mutations at the Fe complex-binding site		
FeGP-C176A	2.2 ± 0.5	1.6±0.2
[Fe]-C176A	ND[1]	ND
[Mn]-C176A	0.12±0.19	0.04±0.04
[Mn]-T13V_C176A_D251A	ND	ND
[Mn]-Mtd	ND	ND

The error bars represent standard deviation.

[1] ND: Not detected (the specific activity was less than 0.015 U/mg).